Droop-Boost Control for Single-Phase Hybrid Power Filter

Jing-Jing Sheng, NingYi Dai, Man-Chung Wong, Chi-Seng Lam, KengWeng Lao

Faculty of Science and Technology
University of Macau, Macau, PR China
mb35439@umac.mo

Abstract—**Hybrid power filter (HPF) is used as a low-cost solution to provide reactive power compensation in distribution systems. It can provide reactive power compensation with a very low operational voltage. Direct current tracking with hysteresis PWM is widely used for controlling the HPF. However, hysteresis PWM suffers from variable switching frequency and high current ripple. Droop control is able to generate reference voltage for controlling the inverter directly from the power to be transferred. With a reference voltage, carrier-based PWM can be applied to the HPF. The droop control is applied to HPF for the first time in this paper. In contrast with conventional droop control, a droop-boost combined control scheme is proposed. The power flow control characteristic of HPF is analyzed to deduce the key parameters for achieving droop-boost control. The control system and the parameter design are conducted and verified by simulation results.**

Keywords—droop control, droop-boost control, hybrid power filter, reactive power compensation;

I. INTRODUCTION

Reactive power compensation can improve system power factor and reduce losses [1][2].The typical configuration of the single phase active power filter (APF) is shown in Fig. 1(a). The single-phase hybrid power filter (HPF) is shown in Fig. 1(b). The HPF can achieve reactive power compensation with a low operational voltage. As a result, the initial inverter voltage rating, the dc capacitor rating and the switching losses are all reduced [3]-[5].

Most of the control methods in HPF use the instantaneous power theory to generate the compensating current, and hysteresis PWM to achieve direct current tracking. The hysteresis PWM suffers from variable switching frequency and high current ripples. If a simple method could be used to generate reference voltage for controlling the inverter, carrier-based PWM could be applied.

Droop control has been widely used in controlling grid-connected inverters. It controls active power and reactive power by adjusting phase angle and amplitude of the inverter output voltage [6]-[8]. In the literature, the droop method is also called independent, autonomous, or wireless control. This method is based on a well-known concept in large-scale power systems, which consists of drooping the frequency of the ac generator when its output power increases. In the case of parallel grid-connected inverters, the active and reactive powers supplied to the ac bus are sensed and averaged, and the resulting signals are used to adjust the frequency and amplitude of the inverter output-voltage reference. Higher reliability and flexibility can be achieved by droop control since it only uses local voltage and current measurements.

Meanwhile, reactive power control and harmonic compensation are also achieved by droop control when it is used to control conventional grid-connected inverter. The APF in Fig.1 (a) is one of the typical configuration of the grid-connected inverter, in which the coupling impedance is an inductor. Until now, droop control has not been applied to a grid-connected inverter, which has a configuration as HPF in Fig. 1(b). When HPF operates, it is mainly controlled for reactive power compensation. Small amount of active power flows between inverter and grid at the same time for DC link voltage control. Therefore droop control is considered to be applied into HPF to generate the reference voltage in this paper.

In this paper, the power flow control characteristic of the HPF is analyzed. A droop-boost control is proposed for the HPF. The parameter design is provided and the simulations are conducted to verify the control method proposed in this paper.

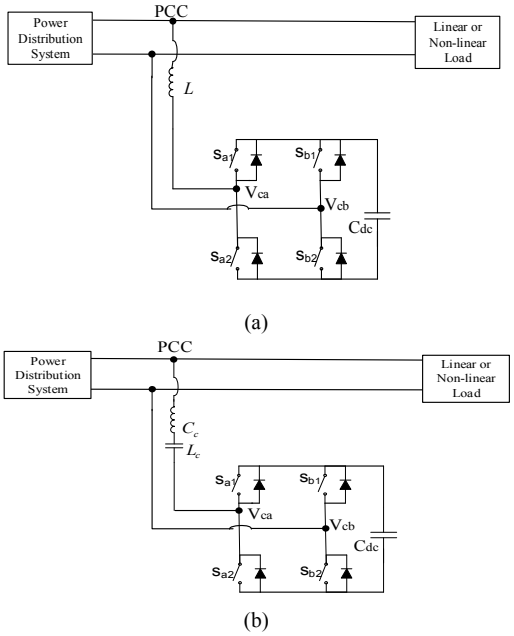

Project supported by Macau Science and Technology Fund (FDCT072/2012/A3) and the University of Macau (MRG014/DNY/2013/FST and MYRG2015-00084-FST)

978-1-4799-8641-5/15/$31.00©2015 IEEE

Fig. 1 (a) Single-phase active power filter (b) Single-phase hybrid filter

II. POWER FLOW ANALYSES FOR SINGLE-PHASE APF AND HPF

Fig. 2 shows the equivalent circuit of the APF and HPF. $v_s = V_s\angle 0^\circ$ is the grid side voltage, $v_{inv} = E\angle\delta$ is the inverter output voltage, ΔV is the voltage drop across the coupling impedance. HereI $= I_P + jI_Q$, I_P is the active injecting current, and I_Q is the reactive compensating current. From the figure of APF and HPF, the coupling impedance is written as (1) and (2).

$$X_L = \omega L, \theta = 90^\circ \quad (1)$$

$$X_C = \frac{1}{\omega C_c} - \omega L_c, \theta = -90^\circ \quad (2)$$

Where X and θ represent the magnitude and phase angle of coupling impedance, respectively. ω is fundamental frequency of utility grid, X_L represents the coupling impedance of the APF, and *Xc* represents the equivalent capacitance of coupling branch in HPF.

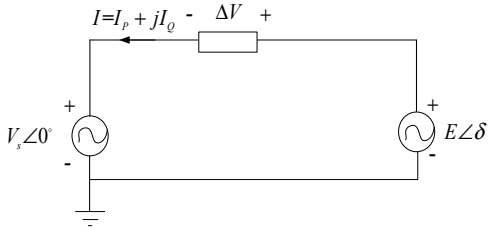

Fig. 2 Equivalent circuit of APF and HPF

The power flow between the grid and the inverter is expressed as:

$$P = \left(\frac{EV_s}{Z}\cos\delta - \frac{V_s^2}{Z}\right)\cos\theta + \frac{EV}{Z}\sin\delta\sin\theta \quad (3)$$

$$Q = \left(\frac{EV_s}{Z}\cos\delta - \frac{V_s^2}{Z}\right)\sin\theta - \frac{EV}{Z}\sin\delta\cos\theta \quad (4)$$

The S_{base} is defined for APF and HPF, as shown in Eq. (5) and (6).

$$S_{base\_L} = \frac{V_s^2}{X_L} = \frac{V_s^2}{\omega L} \quad (5)$$

$$S_{base\_C} = \frac{V_s^2}{X_C} = V_s^2 \cdot \omega C \quad (6)$$

Thus, for a APF, the inverter output voltage parameters can be obtain as Eq. (7) and (8) to describe the power flow characteristics.

$$P/S_{base\_L} = \frac{E}{V_s}\sin\delta \quad (7)$$

$$Q/S_{base\_L} = \frac{E}{V_s}\cos\delta - 1 \quad (8)$$

For HPF, the inverter output voltage parameters can be obtained as Eq. (9) and (10).

$$P/S_{base\_C} = -\frac{E}{V_s}\sin\delta \quad (9)$$

$$Q/S_{base\_C} = 1 - \frac{E}{V_s}\cos\delta \quad (10)$$

Both active and reactive power vary in terms of the RMS value of inverter output voltage E and its phase angle δ, as shown in Fig.3.

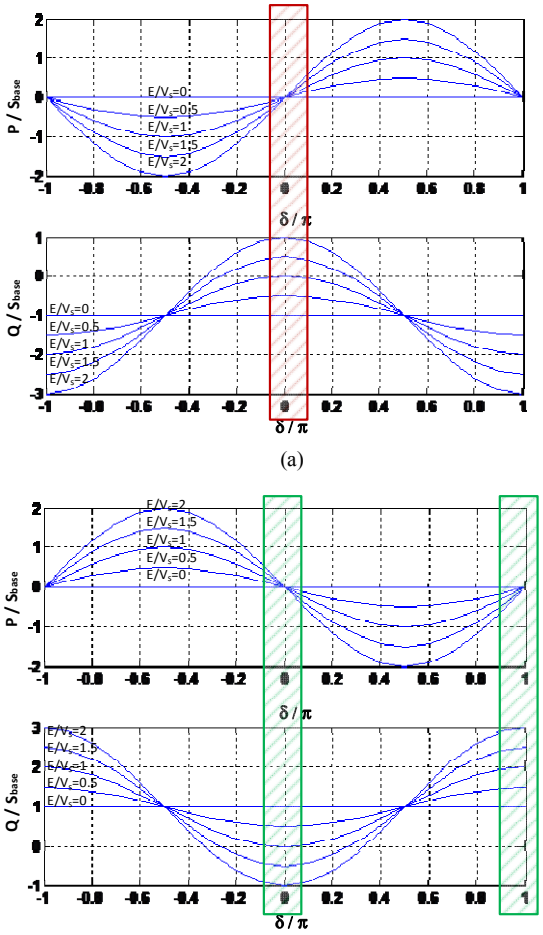

(a)

(b)

Fig. 3 Normalized power flow of (a) APF (b) HPF

The comparison between APF and HPF is expressed as follow,

- In APF, inverter output voltage can be lower than grid voltage when compensating capacitive load;
- In HPF, inverter output voltage can be lower than grid voltage when compensating inductive load;

For the APF, if the operational voltage is high enough, the reactive power could vary in a range of $-S_{base\_L}$ to $+S_{base\_L}$ when δ is zero. Hence, the linearization of the droop control is done in the vicinity of this point. However, the main advantage of the HPF is that it is able to compensate reactive power of inductive load with a low operational voltage. In this paper, the power flow control range of the HPF is limited to the area that only require an operational voltage, which is lower than the grid side voltage. This area is marked in Fig. 3(b). In order to fully utilize the reactive power compensation range, the phase angle δ may be controlled around zero or 180 degrees. As a result, the linearization to deduce droop control is done at both of these two points in the next Section.

III. PROPOSED DROOP-BOOST CONTROL FOR SINGLE-PHASE HPF

Detailed deduction of the proposed droop-boost control method for single-phase HPF is introduced in this section. Firstly, the linearization of power flow for deducing the droop-boost control is discussed in this part. Secondly, the droop coefficients *m* and *n* will be defined based on the active power injection and reactive power compensation along with the given approximation limitation. Finial, the simple comparison between APF and HPF will be provided at the end of this part.

A. Linearization of power flow

In order to deduce the linearization formula for the HPF, the partial derivative of active power and reactive power in terms of phase angle is provided in Eq. (11) and (12), and also the partial derivative of active power and reactive power in terms of *E* is provided in Eq. (13) and (14).

$$\frac{\partial(\mathrm{P}/S_{base\_C})}{\partial\delta} = -\frac{\mathrm{E}}{\mathrm{V_s}}\cos\delta \quad (11)$$

$$\frac{\partial(\mathrm{Q}/S_{base\_C})}{\partial\delta} = \frac{\mathrm{E}}{\mathrm{V_s}}\sin\delta \quad (12)$$

$$\frac{\partial(\mathrm{P}/S_{base\_C})}{\partial E} = -\frac{1}{\mathrm{V_s}}\sin\delta \quad (13)$$

$$\frac{\partial(\mathrm{Q}/S_{base\_C})}{\partial E} = -\frac{1}{\mathrm{V_s}}\cos\delta \quad (14)$$

TABLE I and TABLE II show the partial derivative of active and reactive power in terms of phase angle and amplitude of inverter output voltage when δ=0 degree and δ=180 degrees. When making linearization at δ=0 degree, it shows that P does not depend on E since in this time $\frac{\partial(\mathrm{P}/S_{base\_C})}{\partial E} \approx 0$. However, *P*/δ shows a droop relationship since $\frac{\partial(\mathrm{P}/S_{base\_C})}{\partial\delta} \approx -\frac{\mathrm{E}}{\mathrm{V_s}} < 0$ as shown in table I. The similar things happened when talking about Q/E relation and also the δ=180 degrees case, which can be seen in TABLE II.

TABLE I
PARTIAL DERIVATIVE OF ACTIVE AND REACTIVE POWER IN TERMS OF PHASE ANGLE AND AMPLITUDE OF INVERTER OUTPUT VOLTAGE WHEN δ=0 degree

Partial derivative	Value	Conclusion
$\frac{\partial(\mathrm{P}/S_{base\_C})}{\partial E}$	≈ 0	*P*/δ droop relationship
$\frac{\partial(\mathrm{P}/S_{base\_C})}{\partial\delta}$	$\approx -\frac{\mathrm{E}}{\mathrm{V_s}} < 0$	
$\frac{\partial(\mathrm{Q}/S_{base\_C})}{\partial E}$	$\approx -\frac{1}{\mathrm{V_s}} < 0$	*Q/E* droop relationship
$\frac{\partial(\mathrm{Q}/S_{base\_C})}{\partial\delta}$	≈ 0	

TABLE II
PARTIAL DERIVATIVE OF ACTIVE AND REACTIVE POWER IN TERMS OF PHASE ANGLE AND AMPLITUDE OF INVERTER OUTPUT VOLTAGE WHEN δ=180 degrees

Partial derivative	Value	Conclusion
$\frac{\partial(\mathrm{P}/S_{base\_C})}{\partial E}$	≈ 0	*P*/δ boost relationship
$\frac{\partial(\mathrm{P}/S_{base\_C})}{\partial\delta}$	$\approx \frac{\mathrm{E}}{\mathrm{V_s}} > 0$	
$\frac{\partial(\mathrm{Q}/S_{base\_C})}{\partial E}$	$\approx \frac{1}{\mathrm{V_s}} > 0$	*Q/E* boost relationship
$\frac{\partial(\mathrm{Q}/S_{base\_C})}{\partial\delta}$	≈ 0	

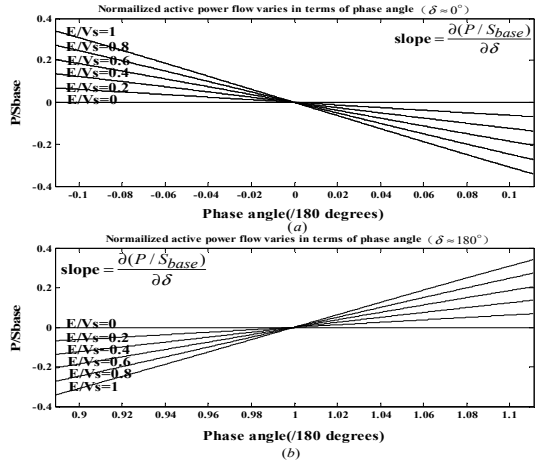

Fig. 4 Normalized active power flow varies in terms of E when phase angle value is chosen around: (a) δ=0 degree and (b) δ=180 degrees

For a clearer explanation, Fig. 4 was provided to show the relation between P and δ around 0 degree (Fig. 4(a)) and 180 degrees (Fig. 4(b)) in different E/Vs conditions. It can be concluded from Fig. 6 that in a small range of δ, active power has a linear relation with δ. Fig. 5 was obtained to show the relation between Q and E around 0 degree (Fig. 5 (a)) and 180 degrees (Fig. 5 (b)) in different δ conditions. It is obvious that in a small range of δ, reactive power has a linear relation with E.

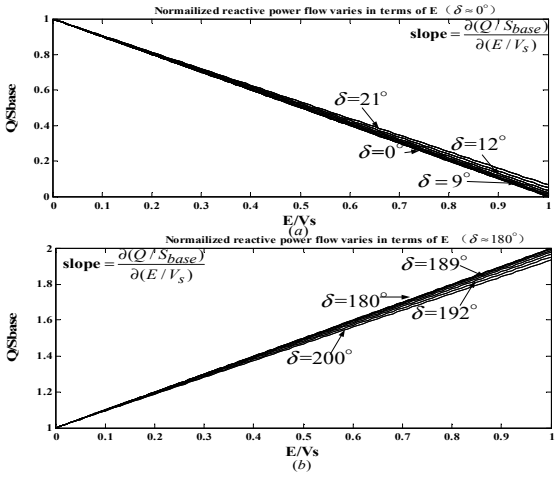

Fig. 5 Normalized reactive power flow varies in terms of E when phase angle value is chosen around: (a) δ=0 degree and (b) δ=180 degrees

The comparison between the conventional and proposed droop method is provided in Fig. 6 and Fig. 7.The proposed droop-boost control uses two operational phase angles for the HPF, which is different from the conventional droop method.

TABLE III
DROOP COMNTROL COMPARISON BETWEEN APF AND HPF

	APF Droop control	HPF Droop-Boost control
Droop function	$\begin{cases}\omega=\omega^*-mP\\E=E^*-nQ\end{cases}$ $(m>0,n>0,E^*=V_s)$	$\begin{cases}\delta=-mP\\E=E^*-nQ\end{cases}$ or $\begin{cases}\delta=mP+180^\circ\\E=-E^*+nQ\end{cases}$ $(m>0,n>0,E^*=V_s)$
Active power	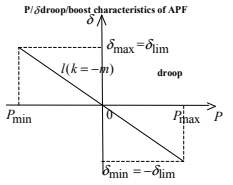	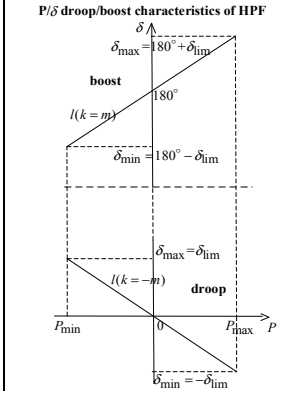
Reactive power	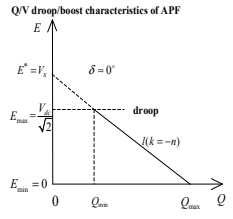	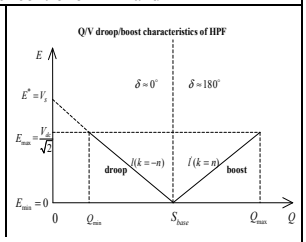

Fig. 6 Active power control of APF and HPF

Fig. 7 Reactive power control of APF and HPF

B. Reactive power-RMS voltage droop/boost coefficient: n

Because the inverter output voltage is determined by DC link voltage, so the control range of the RMS value of inverter output voltage is 0 ~E_{max}, yields,

$$\Delta E_{max} = E_{max} - 0 = \frac{V_{DC}}{\sqrt{2}} \tag{15}$$

The minimum and maximum value of reactive power compensation is gotten according to the initial power flow equations when δ=0 and δ=180 degrees, then obtained the reactive power range:

$$Q_{range} = Q_{max} - Q_{min} = \left(1+\frac{V_{DC}}{\sqrt{2}V_S}\right)\cdot S_{base} - \left(1-\frac{V_{DC}}{\sqrt{2}V_S}\right)\cdot S_{base} = \frac{2V_{DC}}{\sqrt{2}V_S}\cdot S_{base} \tag{16}$$

Thus, the amplitude voltage droop/boost is gotten by substituting Eq. (15), (16),

$$\mathrm{n} = \frac{\Delta E_{max}}{\frac{1}{2}Q_{range}} = \frac{V_S}{S_{base}} = \frac{X_C}{V_S} \tag{17}$$

C. Active power-phase droop/boost coefficient: m

The variation of phase angle needs to be very small to guarantee not only the accuracy of the approximation of the power flow equation, but the reactive power decoupling. Because when variation of phase angle is big, such as 20 degrees in Fig. 5, the linearization comes to a bad performance and the reactive power droop is influenced deeply. So the variation of phase angle is limited. When phase angle changing clockwise around δ=0, active power output value varies from P_{max} to P_{min}; when phase angle changing clockwise around δ=180, active power output value varies from P_{min} to P_{max}. This two cases determine the two equations of phase angle droop/boost characteristics as shown in proposed droop functions. Noting that active power variation range is so smaller compared with reactive power when considering the limitation of phase angle, the droop coefficient is deduced as following. Assuming that phase angle changes from $-\delta_{lim}$ to δ_{lim}, i.e.,

$$\Delta\delta_{max} = 2\delta_{lim} \tag{18}$$

And active power range can be obtained according initial power equation when d=0 for example,

$$P_{range} = 2\frac{EV_S}{X_C}\delta_{lim} = \frac{2E\delta_{lim}}{V_S}S_{base} \tag{19}$$

Define phase angle droop coefficient in Eq. (20)

$$m = \frac{\Delta\delta_{max}}{P_{range}} = \frac{X_C}{EV_S} = \frac{n}{E} \tag{20}$$

Fig. 8 shows the control block diagram of the whole system, which consists of a dc link voltage control, a droop/boost control a PWM unit. The output signal of dc link voltage control generates the active power input for the droop-boost controller. Its reactive power input is calculated from the reactive power of the loading. The output of droop-boost controller is a voltage reference, which is sent to the carrier-PWM unit to control the converter.

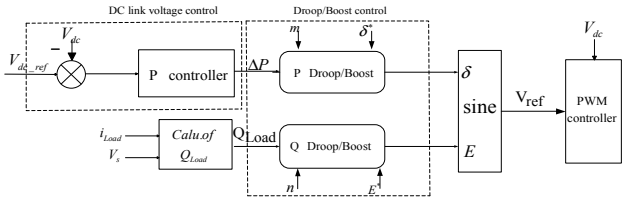

Fig. 8 Control block diagram of the whole system

IV. Simulation Results

The verification of this proposed droop-boost control method is verified in the two steps, first compare the proposed droop function with initial power flow equations, and then verified the droop method in PSCAD simulation. Here the HPF parameters with proposed droop control is shown in TABLE IV. For the different power injection, the theoretical value and the droop/boost value of δ and E are obtained according to equations in TABLE III.

TABLE IV
CGCI PARAMETERS WITH DROOP CONTROLLER FOR SIMULATIONS

System parameters			Physical values
Source side	Source voltage	V_s	220V
	System frequency	f	50Hz
HPF	DC link voltage	V_{dc}	141V
	Power base		1100VA
	Reactive power range	Q_{range}	1000Var
	Active power range	P_{range}	200W
	Coupled capacitor	C	71uf
	Coupled inductor	L	8mH
Droop controller	Amplitude voltage droop coefficient	n	0.193
	Phase angle droop coefficient	m_{max}	0.23
Linear loading	1th inductive loading	Q_{Load1}	1430.1Var
	2th inductive loading	Q_{Load2}	820.33Var

From the TABLE V, according to the different active and reactive power injection, the δ and E can be obtained through the theoretical function and droop-boost function. The difference is calculated around less than 5%, which is acceptable in these selected cases. So this table verifies that the proposed droop-boost control method works well in the HPF system.

TABLE V
DROOP/BOOST CONTROL VERIFICATION BY COMPARING WITH THEORETICAL CALCULATION

Power injection		Theoretical value		Droop-boost method		Difference	
$P_{ref}(W)$	Q_{ref}(Var)	δ	E(V)	δ	E(V)	Δδ(%)	ΔE(%)
40	900	-9.3428	47.4199	-9.20	46.3	1.53%	2.36%
80	1600	189.932	89.2651	198.4	88.8	4.46%	0.52%

The simulation is conducted by using PSCAD. The system configuration is as shown in Fig. 1(b). In the simulation, single-phase HPF starts operation at 0.1s with the 1st inductive loading. At 1.2s, the 2nd inductive loading is connected and the 1st loading is disconnected. The reactive power of the loading is reduced. Fig. 9(a) shows that output reactive power of the HPF tracks the reactive power of the loads. The dc voltage is kept stable by controlling small active power flow by using the proposed droop-boost method. Fig. 9(b) shows the voltage reference generated by the droop-boost controller and the source current and load current. TABLE VI summarize the system performance in simulation results.

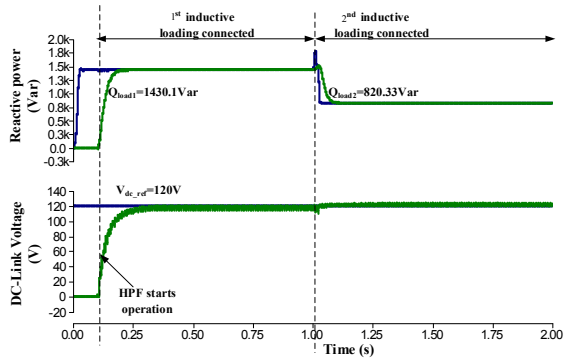

(a)

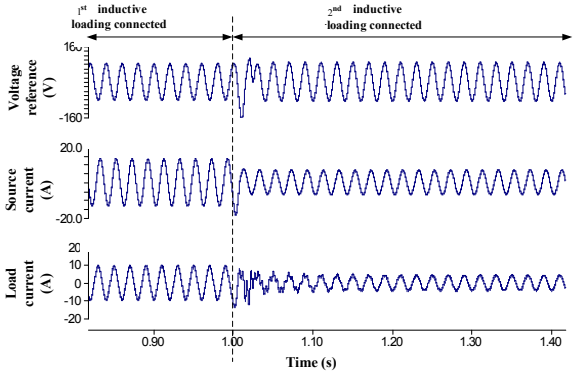

(b)

Fig. 9 Simulation result (a) Reactive power injection and DC link voltage (b) Waveform of voltage reference, source current and load current

TABLE VI
SIMULATION RESULTS BEFORE AND AFTER SPHF OPERATION

	Before HPF Operation			After HPF Operation			
	Q_{Load}(Var)	DPF	$i_s(A_{rms})$	Q_s(Var)	DPF	$i_s(A_{rms})$	THD_{is}(%)
1st load	1430.1	0.71	9.25	-5	1	6.59	3.09
2nd load	820.33	0.63	4.80	-2	1	3.04	2.44

V. CONCLUSIONS

A droop-boost control method is proposed for single-phase HPF. In contract with conventional control method for the HPF, the proposed method generates voltage reference directly from the power flow. There is no need to calculate current reference signal and carrier-based PWM can be applied. In order to fully utilize the controllable reactive power output range of the HPF, the proposed droop-boost control uses two operational phase angle for the inverter. The validity of the proposed control method is verified by simulation results.

REFERENCES

[1] H. Akagi, "Trends in active power line conditioners," *IEEE Trans. Power Electron.*, vol. 9, no. 3, pp. 263–268, 1994.

[2] R. S. Herrera, P. Salmeron, and H. K. H. Kim, "Instantaneous Reactive Power Theory Applied to Active Power Filter Compensation: Different Approaches, Assessment, and Experimental Results," IEEE Trans. Ind. Electron., vol. 55, no. 1, 2008.

[3] Dai, N., Zhang, C., Wong, M., Guerrero, J. M., & C.-S. Lam, "Analysis, control and experimental verification of a single-phase capacitive-coupling grid-connected inverter," IET Power Electron., vol. 10.1049/ie, p. 0373, 2014.

[4] C. L. M. W. Y. Han, "Hysteresis current control of hybrid active power filters," no. December 2011, pp. 1175–1187, 2012.

[5] C.-S. Lam, W.-H. Choi, M.-C. Wong, and Y.-D. Han, “Adaptive DC-Link Voltage-Controlled Hybrid Active Power Filters for Reactive Power Compensation,” vol. 27, no. 4, pp. 1758–1772, 2012.
[6] J. Kim, J. M. Guerrero, S. Member, P. Rodriguez, and R. Teodorescu, “Output Impedances for an Inverter-Based Flexible AC Microgrid,” vol. 26, no. 3, pp. 689–701, 2011.
[7] J. Quesada, J. A. Sainz, R. Sebastian, and M. Castro, “Decoupled droop control techniques for inverters in low-voltage AC microgrids,” 2014 IEEE 11th Int. Multi-Conference Syst. Signals Devices, SSD 2014, pp. 1–6, 2014.
[8] H. Han, Y. Liu, Y. Sun, M. Su, and J. M. Guerrero, “An Improved Droop Control Strategy for Reactive Power Sharing in Islanded Microgrid,” IEEE Trans. Power Electron., vol. 30, no. 6, pp. 3133–3141, 2015.
[9] J. M. Guerrero, L. G. de Vicuna, J. Matas, M. Castilla, and J. Miret, “A wireless controller to enhance dynamic performance of parallel inverters in distributed generation systems,” IEEE Trans. Power Electron., vol. 19, no. 5, pp. 1205–1213, 2004.
[10] Engler and N. Soultanis, “Droop control in LV-grids,” 2005 Int. Conf. Futur. Power Syst., 2005.
[11] H. W. H. Wang, X. Y. X. Yue, X. P. X. Pei, and Y. K. Y. Kang, “A new method of power calculation based on parallel inverters,” 2009 IEEE 6th Int. Power Electron. Motion Control Conf., 2009.
[12] J. M. Guerrero, L. G. De Vicuña, J. Matas, J. Miret, and M. Castilla, “Output impedance design of parallel-connected UPS inverters,” IEEE Int. Symp. Ind. Electron., vol. 2, no. 4, pp. 1123–1128, 2004.
[13] J. M. Guerrero, J. Matas, L. G. De Vicuña, M. Castilla, and J. Miret, “Wireless-control strategy for parallel operation of distributed-generation inverters,” IEEE Trans. Ind. Electron., vol. 53, no. 5, pp. 1461–1470, 2006.
[14] J. M. Guerrero, N. Berbel, J. Matas, J. L. Sosa, J. Cruz, and A. Alentorn, “Decentralized Control for Parallel Operation of Distributed Generation,” vol. 54, no. 2, pp. 1–10, 2007.
[15] H. Liao and C. S. Wu, “A voltage stability droop control strategy of wireless parallel inverters,” Proc. - Int. Conf. Electr. Control Eng. ICECE 2010, pp. 4978–4981, 2010.

978-1-4799-8641-5/15/$31.00©2015 IEEE